NANO LETTERS

Letter

pubs.acs.org/NanoLett

Molecular Materials for Nonaqueous Flow Batteries with a High Coulombic Efficiency and Stable Cycling

Margarita Milton,[†] Qian Cheng,[‡] Yuan Yang,[*,‡] Colin Nuckolls,[*,†,§] Raúl Hernández Sánchez,[*,†] and Thomas J. Sisto[*,†,§]

[†]Department of Chemistry, [‡]Department of Applied Physics and Applied Mathematics, Columbia University, New York, New York 10027, United States

[§]Institute of Advanced Materials and Nanotechnology, the State Key Laboratory of Refractories and Metallurgy, School of Chemistry and Chemical Engineering, Wuhan University of Science and Technology, Wuhan 430081, China

Supporting Information

ABSTRACT: This manuscript presents a working redox battery in organic media that possesses remarkable cycling stability. The redox molecules have a solubility over 1 mol electrons/liter, and a cell with 0.4 M electron concentration is demonstrated with steady performance >450 cycles (>74 days). Such a concentration is among the highest values reported in redox flow batteries with organic electrolytes. The average Coulombic efficiency of this cell during cycling is 99.868%. The stability of the cell approaches the level necessary for a long lifetime nonaqueous redox flow battery. For the membrane, we employ a low cost size exclusion cellulose membrane. With this membrane, we couple the preparation of nanoscale macromolecular electrolytes to successfully avoid active material crossover. We show that this cellulose-based membrane can support high voltages in excess of 3 V and extreme temperatures (−20 to 110 °C). These extremes in temperature and voltage are not possible with aqueous systems. Most importantly, the nanoscale macromolecular platforms we present here for our electrolytes can be readily tuned through derivatization to realize the promise of organic redox flow batteries.

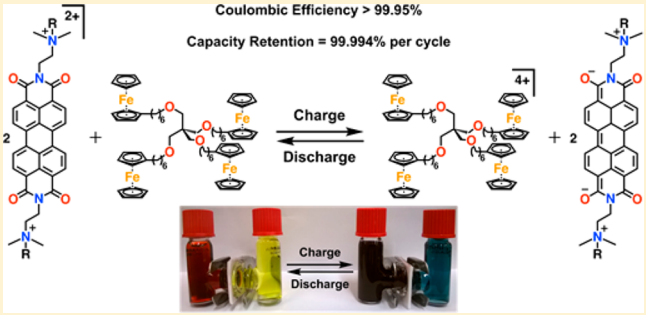

KEYWORDS: *Redox flow battery, organic electrolyte, perylene diimide, size-exclusion membrane, ferrocene*

This manuscript describes a working battery comprised of all organic electrolytes dissolved in organic media that has an outstanding long-term cycling stability. Renewable power generation has been rising steadily and is an ever-increasing need for an energy secure future. Specifically, 60% of all new energy produced between now and 2040 is predicted to come from solar and wind generation.[1] To cope with the intermittency of these energy resources, efficient and durable energy storage devices must be developed.[2] To meet this need, redox flow batteries (RFBs, Figure 1a) are an attractive technology, and their aspects are broadly covered in a number of reviews.[3−5] In RFBs, the storage electrolytes are dissolved in solvent, stored in tanks, and pumped through an electrochemical cell. Notably, a RFB decouples power and capacity, and they can be varied independently with power relying on the cell stack and storage capacity depending on the tank size. Since their proposal in 1949[6] and later implementation,[7−9] there have been remarkable strides in high performance RFBs, the most developed of which are aqueous systems which employ water as a solvent.[10−13] The benefits of aqueous systems are inexpensive salts and their resultant high conductivity in water. Despite this progress on RFBs, no long-term stable RFB in organic media has been reported to date due to the instability of the charged electrolytes.[14−22] While several studies in organic media have shown relative stability (∼25% loss over ∼150 cycles), these cycling experiments represent no more than a few days. Realistically, batteries must store energy in their charged state over periods of time. Therefore, it is important to develop electrolytes that display long calendar stability in their charged state as well as cycling capacity retention. One clear advantage of using organic over aqueous media is the higher energy and power density accessed through the larger electrochemical window, thus shrinking the footprint of organic flow batteries.[23] This benefit has been showcased through the development of high-voltage, high-energy density hybrid batteries that utilize lithium metal or intercalated lithium graphite electrodes coupled to a flow half cell.[24−27] However, in these types of systems the power and capacity are not fully decoupled. Therefore, to realize scalable RFBs, it is essential to move away from solid electrodes.

In the study presented here, we address an unmet need for organic RFBs by designing and synthesizing stable organic compounds that are easily tuned through derivatization, along

Received: September 25, 2017
Revised: October 17, 2017
Published: November 10, 2017

Downloaded via COLUMBIA UNIV on August 20, 2018 at 21:25:46 (UTC).
See https://pubs.acs.org/sharingguidelines for options on how to legitimately share published articles.

ACS Publications © 2017 American Chemical Society

DOI: 10.1021/acs.nanolett.7b04131
Nano Lett. 2017, 17, 7859−7863

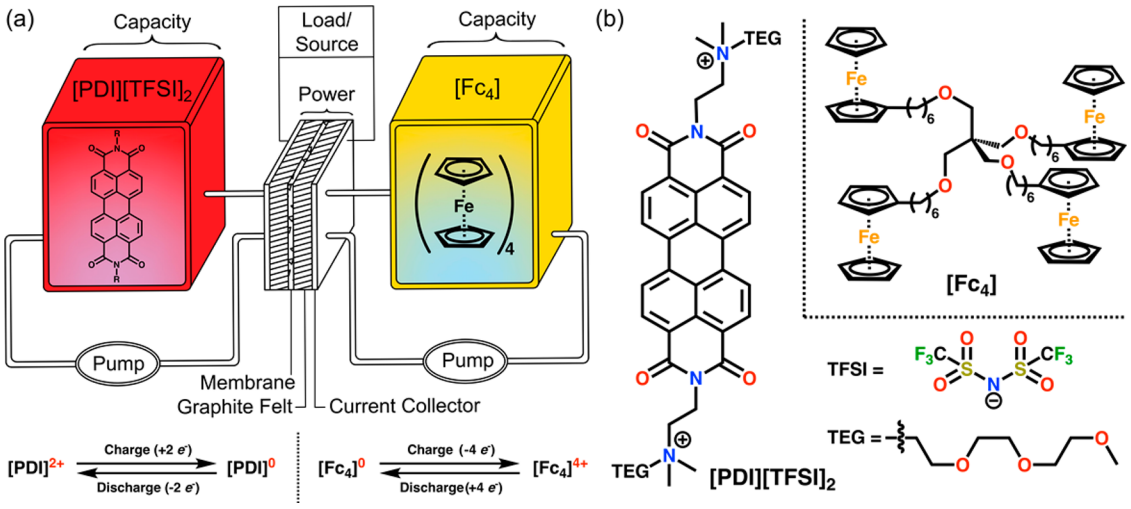

Figure 1. (a) Schematic of a redox flow battery. Redox reactions for $[PDI][TFSI]_2$ and $[Fc_4]$ are displayed for the charging and discharging processes. (b) Structure of the active electrolytes employed in this study.

with engineering a battery that displays remarkable calendar and capacity retention. These compounds and membrane provide a core platform for future synthesis toward realizing truly stable RFB at higher voltages. Recently, several studies have explored organic electrolytes using half-cells, in which a positive or negative electrolyte is tested for stability ex situ, outside of the context of a full battery.[19,28,29] In this report, we provide the first example of a long-term stable working battery with both electrolytes fully dissolved in organic media. We describe here two new redox pairs soluble in organic solvent (Figure 1b), one for the negative electrode of the battery based on a derivative of perylene diimide (PDI) ($[PDI][TFSI]_2$) and another for the positive electrode based on a ferrocene derivative ($[Fc_4]$). The ferrocene derivative showcases the viability of using a nanoscale macromolecular strategy to prevent membrane crossover, and the $[PDI][TFSI]_2$ has a solubilizing TEG (TEG = $(CH_2CH_2O)_3CH_3$) chain that highlights the ease of synthetic manipulability in this class of electrolytes. The solubility of these molecules is equivalent to >1 mol electron/liter, and steady performance >450 cycles is observed in cells with a concentration of 0.4 mol electron/liter. Although nonaqueous RFBs with lithium at one electrode have utilized molecules with higher energy densities,[30,31] 0.4 M is among the highest concentrations reported in redox flow batteries with two organic electrolytes dissolved in organic media. Finally, we demonstrate that the cellulose-based membrane can support high voltages (>3 V) in an organic redox flow battery and can operate at extreme temperatures (−20 to 110 °C). At the same time this membrane displays extremely low permeability of the organic electrolytes employed herein.

For a redox flow cell, it is important to design the membrane and the active molecules in concert because ion crossover and membrane degradation are critical to the performance of RFBs.[32] Furthermore, a potential membrane for organic media must be inexpensive and able to reliably prevent crossover of the active components at a variety of voltages and temperatures. We found that a dialysis, size exclusion membrane made from cellulose was suitable for fulfilling these needs.[12] To partner with this membrane, we synthesized $[PDI][TFSI]_2$ and nanoscale macromolecular tetraferrocene species $[Fc_4]$ (Figure 1b) as the active components for the negative and positive half cells, respectively. Their syntheses and characterization can be found in the Supporting Information (SI). They were designed to have large hydrodynamic radii to preclude their ability to transverse the dialysis membrane. A similar strategy has been employed for polymers[12] and oligomers.[33] Perylene diimide is an ideal platform as an anolyte molecule due to its accessible two-electron reduced state, chemical stability as a radical anion,[34] and its straightforward derivatization.[35] As a case in point, $[PDI][TFSI]_2$ was easily synthesized as a double tetra-alkyl ammonium salt with a glycol chain, showcasing the ease of derivatization to achieve higher solubility. This synthetic tunability provides access to a concentration of >1 M electron in acetonitrile, which corresponds to a theoretical capacity of 26.8 A h/L. Likewise, ferrocene, one of the pillars of organometallic redox chemistry, has a well-known oxidation−reduction couple and is easily derivatized.[36] Neutral $[Fc_4]$ is a viscous oil, which in diglyme affords a maximum concentration of 2 M (8 M electron due to four subunits) representing a theoretical capacity of 214.4 A h/L.

Figure 2a displays the cyclic voltammogram of a solution containing $[PDI]^{2+}$ and $[Fc_4]$. From these data, we extract the standard open circuit voltage. Mixing these compounds in a 4:1 MeCN:THF (v/v) solvent mixture results in the voltammogram displayed. The two closely spaced[37] electrochemical events situated around −0.7 V vs $Ag^{0/+}$ are the well-known reductions for perylene diimide derivatives.[38] $[Fc_4]$ undergoes a four-electron event (one for each ferrocene unit) at ∼0.15 V vs $Ag^{0/+}$. On the basis of these redox events, the expected standard cell voltage of a battery made from $[PDI]^{2+}$ and $[Fc_4]$ is ∼0.85 V.

With each of the components for a redox flow battery in hand, we test the stability of this system in a static cell (H-cell configuration) employing the dialysis membrane as separator and carbon felt as electrodes. Details for the measurement can be found in the SI. $[Fc_4]$ and $[PDI][TFSI]_2$ were dissolved in 10:1 MeCN−diglyme and loaded in approximately a 2:1 $[PDI][TFSI]_2$:$[Fc_4]$ stoichiometry (i.e., the same electron molarity). We chose lithium hexafluorophosphate and lithium bis(trifluoromethanesulfonyl)imide as two different supporting electrolytes due to their ability to pass through the membrane,[39] as well as their high conductivity in acetonitrile solutions.[40] We operate the low concentration cells at a

DOI: 10.1021/acs.nanolett.7b04131
Nano Lett. 2017, 17, 7859−7863

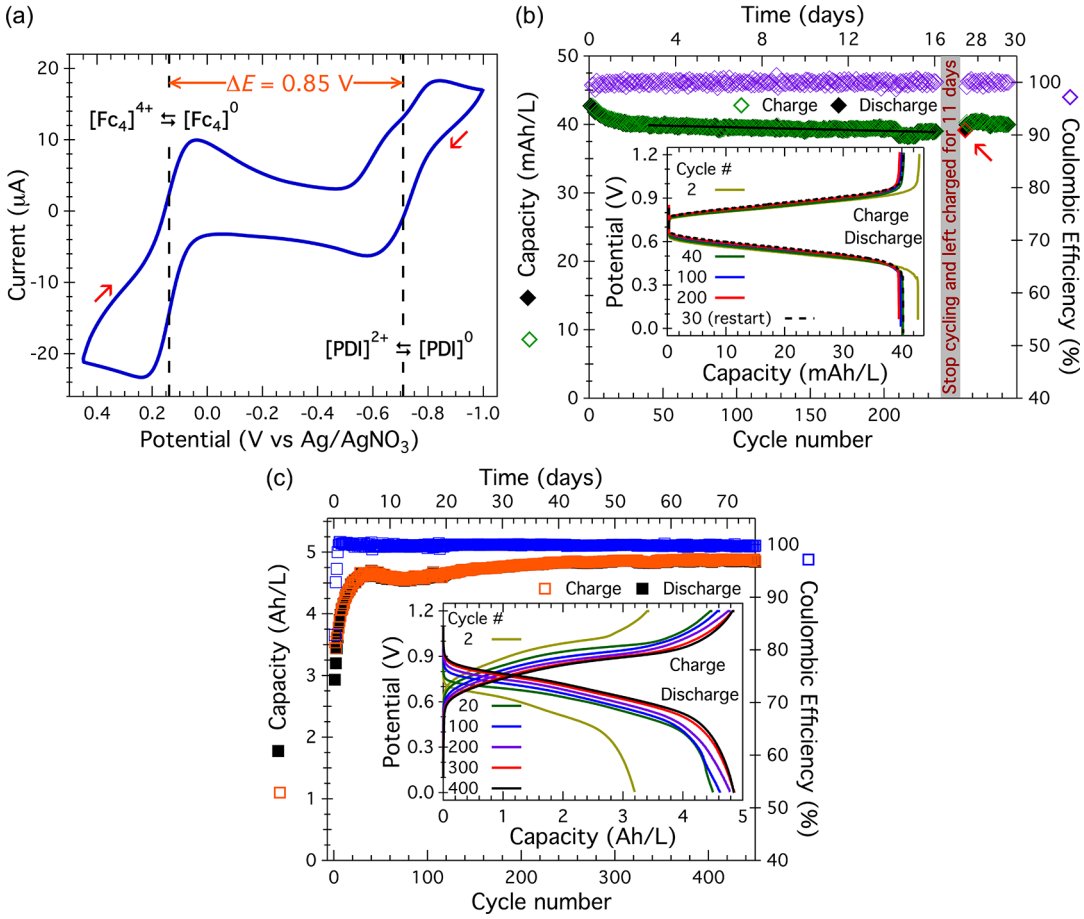

Figure 2. (a) Cyclic voltammetry of $[Fc_4]$ and $[PDI][TFSI]_2$ scanned at 50 mV/s in 4:1 MeCN−THF. 0.1 M $LiPF_6$ was used as supporting electrolyte. (b,c) Cycling data for the battery $[PDI]^0|[PDI]^{2+}||[Fc_4]^{4+}|[Fc_4]^0$. (b) Low concentration cell assembled using 1.17 mM $[Fc_4]$ and 1.8 mM $[PDI][TFSI]_2$. Repeated charge (green diamonds)/discharge (black diamonds) cycling over >230 cycles at 1 C (1.16 mA/cm^2) in a stirred H-cell. The Coulombic efficiency (purple diamonds) is also plotted and has an average of 99.955%. Cycling was paused in the charged state for 11 days. The first discharge (red diamond) and subsequent cycling shows negligible capacity loss. (c) High concentration cell using 0.4 M electron equivalents (0.2 M $[PDI][TFSI]_2$ and 0.1 M $[Fc_4]$). Charge (orange square) and discharge (black square) capacities are shown for >450 cycles corresponding to more than 74 days of operation. The average CE (blue squares) above cycle 5 is 99.868%. In both cells (b,c) Li[TFSI] was used as supporting electrolyte, and the voltage was limited from 0 to 1.2 V. Insets in (b,c) display selected charge and discharge profiles for their corresponding cell.

constant current of 1 C (1.16 mA/cm^2) and cycle repeatedly between charge and discharge while stirring each solution (Figure 2b and S2,3). At this 1 C current, the cell reached >80% state of charge, which is necessary to show cycling stability.[41] The important finding is that the cell is stable. A clear indicator of the stability is the capacity retention over time.[12] In Figure 2b we show the capacity retention for the charge and discharge process over more than 200 cycles. After an initial small decrease in capacity, the charge and discharge capacity settles after cycle 40. Linearly fitting this data from 40 to 235, we obtain a slope representing a fade of 0.00614% per cycle for the discharge capacity. To test for decomposition of the charged active molecules, we stopped a cell in its charged state for 11 days, after which we resumed cycling. The charged molecules, $[PDI]^0$ and $[Fc_4]^{4+}$, remain unaffected as we were able to discharge the full capacity stored (red diamond in Figure 2b). Remarkably, resuming cycling for 30 more charge/discharge cycles we observe no capacity loss (Figure 2b). All told, the radicals formed upon charging the cell are so stable that no decomposition is observed after this cell resided for more than 500 h at 50% or more state of charge.

This stability is unprecedented for a redox flow battery utilizing electrolytes dissolved in organic media. From the charge and discharge capacity at each cycle, we calculate the Coulombic efficiency (CE).[42] The CE is also plotted in Figure 2b and displays an average of 99.955%. This CE value is also remarkable for a redox flow battery with electrolytes dissolved in organic media and approaches those of aqueous systems that have been highly optimized over many years.[10−13,43−45] We measure the cell's open circuit voltage at different states of charge (SOC) and find a monotonic increase from ∼0.63 to ∼0.82 V from 10 to 90% SOC, respectively (Figure S4). Finally, we observe nearly superimposable charge and discharge profiles—another indicator of stability (Figure 2b inset).[13,44] In fact, there is a small shift during the first 40 cycles where the initial capacity of ∼87% SOC settles to ∼81% SOC at around cycle 40. Taken together, this represents the first long-term highly stable solution state battery in organic media.

One important criteria for new organic electrolytes is their stability when charged at high concentration. To address this, we tested high concentration cells by assembling pouch cells (see the SI).[16] Figure 2c shows cycling of a battery built with 0.4 M electron equivalents (0.1 M $[Fc_4]$ and 0.2 M $[PDI][TFSI]_2$). This high concentration rivals state-of-the-art organic media RFBs[46,47] while displaying long-term cycling stability. It has an average CE above cycle 5 of 99.868%. An

DOI: 10.1021/acs.nanolett.7b04131
Nano Lett. 2017, 17, 7859−7863

initial induction period of around 20 cycles is observed due to the insolubility of neutral $[Fc_4]$ in acetonitrile. This leads to a slow rise in capacity due to the time necessary for $[Fc_4]$ to fully penetrate the electrode, as charged $[Fc_4]$ is soluble in acetonitrile. After this induction period, the cell settles at a constant charge/discharge capacity corresponding to ∼81% SOC, akin to the low concentration cell (Figure 2c inset). The charge/discharge profiles of the low and high concentration cells have slightly different shapes due to stirring in the low concentration cell, which leads to low diffusion impedance and a sharp approach toward the cutoff voltages. Once level, the energy efficiency of this high concentration cell is ∼68% measured at cycle 200. Taken together, this cell demonstrates the stability of the compounds at relevant battery operating conditions.

Finally, we sought to test if the membrane will be amenable to large temperature excursions and to higher-voltage second generation compounds. We exposed the membrane to high (110 °C) and low (−20 °C) temperatures, as well as to strong reducing and oxidizing conditions, after which we performed dialysis. The SI contains the details for these experiments. For example, we soaked the membrane in a solution of sodium naphthalenide (approximately −3.0 V vs $Fc^{0/+}$)[48] and subsequently assembled an H-cell with this membrane. One chamber of the H-cell was filled with $[PDI][TFSI]_2$ in acetonitrile,[49] while the other contained pure acetonitrile. After stirring overnight, no detectable crossover of the $[PDI][TFSI]_2$ was visibly observed (Figure 3a). Strongly

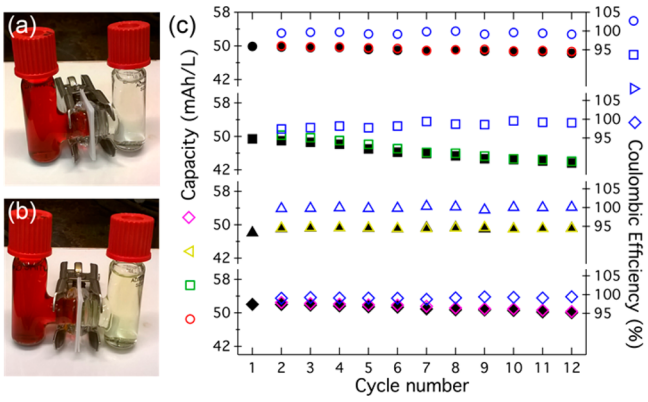

Figure 3. H-cells with $[PDI][TFSI]_2$ and $LiPF_6$ on the left side after treatment with (a) sodium naphthalenide and (b) $NOBF_4$ followed by dialysis for 15 h. (c) Cycling data of four H-cells assembled with membranes treated under the following conditions: sodium naphthalenide (circles), $NOBF_4$ (squares), 110 °C (triangles), and −20 °C (diamonds).

oxidizing ($NOBF_4$, c.a. 0.9 V vs $Fc^{0/+}$)[48] conditions yielded similar results but with a slight fluorescence from crossover of the $[PDI][TFSI]_2$ (Figure 3b). We also find that the membrane is stable at high (110 °C) and low (−20 °C) temperatures (Figures S8−S10). As a point of emphasis, aqueous cells would not be operable at these extreme temperatures.

With this encouraging preliminary data in hand, we next chose to quantitatively assess the impact of these treatments on the membrane's performance under battery operating conditions. Cycling experiments show stable cycling for all conditions tested except for the membrane treated with $NOBF_4$, which shows a small monotonic fade presumably due to crossover of the active electrolytes (Figure 3c). To quantify the amount of crossover seen in these experiments, we took UV−vis spectra of the $[Fc_4]$ chamber. From the molar absorptivity of the strong chromophore $[PDI][TFSI]_2$ (ε_{max} = 76 341 M^{-1} cm^{-1}) we find a crossover of <0.05% for the reducing, hot, and cold conditions, while the oxidizing nitrosonium condition gives a crossover of 1.25% (see SI). Additionally, the low concentration cell above (Figure 2b) was dismantled after cycling and checked for crossover. UV−vis spectroscopy showed that 0.2% of the $[PDI][TFSI]_2$ crossed over during the >30 days and >250 cycles, indicating that crossover is negligible. The key finding is that the cellulose-based membrane is effective in organic solvents over long periods of time, stable to a >3 V voltage window, and stable to temperatures outside the range available for aqueous systems.

In this study, we report the first highly stable battery utilizing electrolytes dissolved in organic media. This battery shows stable cycling for more than a month with a retention of 99.994% per cycle, which is extraordinary. This system also shows a best in class Coulombic efficiency of 99.955%, which is comparable with aqueous systems that have been heavily optimized over years of study. In this work, we also introduce a new organic electrolyte platform to the flow battery field based on perylene diimide cores. The reduced species (radicals) of this family of compounds are exceptionally stable. Drawbacks of this work include the small potential window and solubility that are below that of highly successful aqueous systems. However, these molecules are amenable to synthetic tunability that will enable higher voltages and greater solubility. The membrane chosen for this cell is shown to withstand the conditions necessary for higher voltages (>3 V) and extreme temperature fluctuations not achievable with aqueous systems. Testing with larger quantities of electrolyte in the flowing configuration will further explore the scalability of this novel design and combination of organic electrolytes and membrane.

■ ASSOCIATED CONTENT

Supporting Information

The Supporting Information is available free of charge on the ACS Publications website at DOI: 10.1021/acs.nanolett.7b04131.

Syntheses, experimental procedures, multinuclear NMR spectroscopy, and electrochemical procedures and characterization (PDF)

■ AUTHOR INFORMATION

Corresponding Authors

*Yuan Yang. E-mail: yy2664@columbia.edu.
*Colin Nuckolls. E-mail: cn37@columbia.edu.
*Raúl Hernández Sánchez. E-mail: rh2780@columbia.edu.
*Thomas J. Sisto. E-mail: ts2983@columbia.edu.

ORCID

Margarita Milton: 0000-0003-4121-8156
Yuan Yang: 0000-0003-0264-2640
Colin Nuckolls: 0000-0002-0384-5493
Raúl Hernández Sánchez: 0000-0001-6013-2708

Notes

The authors declare no competing financial interest.

■ ACKNOWLEDGMENTS

The Columbia University Shared Materials Characterization Laboratory was used for this research. We thank Columbia

DOI: 10.1021/acs.nanolett.7b04131
Nano Lett. 2017, 17, 7859−7863

University for this facility. R.H.S. acknowledges the support of the Columbia Nano Initiative Postdoctoral Fellowship. C.N. thanks Sheldon and Dorothea Buckler for their generous support. Q.C. and Y.Y. acknowledge support from startup funding by Columbia University and NSF MRSEC PAS[3] (DMR-1420634). Partial support was provided by the Office of Naval Research under award no. N00014-16-1-2921.

REFERENCES

(1) International Energy Agency. World Energy Outlook 2016. *International Energy Agency* 2016, June 23, 2017.
(2) Yang, Z.; Zhang, J.; Kintner-Meyer, M. C. W.; Lu, X.; Choi, D.; Lemmon, J. P.; Liu, J. *Chem. Rev.* **2011**, *111*, 3577−3613.
(3) Zhao, Y.; Ding, Y.; Li, Y.; Peng, L.; Byon, H. R.; Goodenough, J. B.; Yu, G. *Chem. Soc. Rev.* **2015**, *44*, 7968−7996.
(4) Ding, Y.; Li, Y.; Yu, G. *Chem.* **2016**, *1*, 790−801.
(5) Ding, Y.; Yu, G. *Angew. Chem., Int. Ed.* **2017**, *56*, 8614−8616.
(6) Kangro, W. Verfahren zur Speicherung von elektrischer Energie. German Patent: 914264C, June 28, 1949.
(7) Thaller, L. H. Electrically rechargeable REDOX flow cell. U.S. Patent: 3996064A, August 22, 1976.
(8) Skyllas-Kazacos, M.; Rychcik, M.; Robins, R. G.; Fane, A. G.; Green, M. A. *J. Electrochem. Soc.* **1986**, *133*, 1057−1058.
(9) Skyllas-Kazacos, M.; Grossmith, F. *J. Electrochem. Soc.* **1987**, *134*, 2950−2953.
(10) Huskinson, B.; Marshak, M. P.; Suh, C.; Er, S.; Gerhardt, M. R.; Galvin, C. J.; Chen, X.; Aspuru-Guzik, A.; Gordon, R. G.; Aziz, M. J. *Nature* **2014**, *505*, 195−198.
(11) Lin, K.; Chen, Q.; Gerhardt, M. R.; Tong, L.; Kim, S. B.; Eisenach, L.; Valle, A. W.; Hardee, D.; Gordon, R. G.; Aziz, M. J.; Marshak, M. P. *Science* **2015**, *349*, 1529−1532.
(12) Janoschka, T.; Martin, N.; Martin, U.; Friebe, C.; Morgenstern, S.; Hiller, H.; Hager, M. D.; Schubert, U. S. *Nature* **2015**, *527*, 78−81.
(13) Hu, B.; DeBruler, C.; Rhodes, Z.; Liu, T. L. *J. Am. Chem. Soc.* **2017**, *139*, 1207−1214.
(14) Matsuda, Y.; Tanaka, K.; Okada, M.; Takasu, Y.; Morita, M.; Matsumurainoue, T. *J. Appl. Electrochem.* **1988**, *18*, 909−914.
(15) Li, Z.; Li, S.; Liu, S.; Huang, K.; Fang, D.; Wang, F.; Peng, S. *Electrochem. Solid-State Lett.* **2011**, *14*, A171−A173.
(16) Brushett, F. R.; Vaughey, J. T.; Jansen, A. N. *Adv. Energy Mater.* **2012**, *2*, 1390−1396.
(17) Wang, W.; Xu, W.; Cosimbescu, L.; Choi, D.; Li, L.; Yang, Z. *Chem. Commun.* **2012**, *48*, 6669−6671.
(18) Huang, J.; Su, L.; Kowalski, J. A.; Barton, J. L.; Ferrandon, M.; Burrell, A. K.; Brushett, F. R.; Zhang, L. *J. Mater. Chem. A* **2015**, *3*, 14971−14976.
(19) Kaur, A. P.; Holubowitch, N. E.; Ergun, S.; Elliott, C. F.; Odom, S. A. *Energy Technol.* **2015**, *3*, 476−480.
(20) Ding, Y.; Zhao, Y.; Yu, G. *Nano Lett.* **2015**, *15*, 4108−4113.
(21) Hagemann, T.; Winsberg, J.; Haupler, B.; Janoschka, T.; Gruber, J. J.; Wild, A.; Schubert, U. S. *NPG Asia Mater.* **2017**, *9*, e340.
(22) Ding, Y.; Zhao, Y.; Li, Y.; Goodenough, J. B.; Yu, G. *Energy Environ. Sci.* **2017**, *10*, 491−497.
(23) Darling, R. M.; Gallagher, K. G.; Kowalski, J. A.; Ha, S.; Brushett, F. R. *Energy Environ. Sci.* **2014**, *7*, 3459−3477.
(24) Huang, Q.; Li, H.; Gratzel, M.; Wang, Q. *Phys. Chem. Chem. Phys.* **2013**, *15*, 1793−1797.
(25) Wei, X. L.; Cosimbescu, L.; Xu, W.; Hu, J. Z.; Vijayakumar, M.; Feng, J.; Hu, M. Y.; Deng, X. C.; Xiao, J.; Liu, J.; Sprenkle, V.; Wang, W. *Adv. Energy Mater.* **2015**, *5*, 5.
(26) Jia, C.; Pan, F.; Zhu, Y. G.; Huang, Q.; Lu, L.; Wang, Q. *Sci. Adv.* **2015**, *1*, e1500886.
(27) Ding, Y.; Yu, G. H. *Angew. Chem., Int. Ed.* **2016**, *55*, 4772−4776.
(28) Sevov, C. S.; Fisher, S. L.; Thompson, L. T.; Sanford, M. S. *J. Am. Chem. Soc.* **2016**, *138*, 15378−15384.
(29) Sevov, C. S.; Samaroo, S. K.; Sanford, M. S. *Adv. Energy Mater.* **2017**, *7*, 1602027.
(30) Wei, X.; Xu, W.; Vijayakumar, M.; Cosimbescu, L.; Liu, T.; Sprenkle, V.; Wang, W. *Adv. Mater.* **2014**, *26*, 7649−7653.
(31) Cosimbescu, L.; Wei, X.; Vijayakumar, M.; Xu, W.; Helm, M. L.; Burton, S. D.; Sorensen, C. M.; Liu, J.; Sprenkle, V.; Wang, W. *Sci. Rep.* **2015**, *5*, 14117.
(32) Su, L.; Darling, R. M.; Gallagher, K. G.; Xie, W.; Thelen, J. L.; Badel, A. F.; Barton, J. L.; Cheng, K. J.; Balsara, N. P.; Moore, J. S.; Brushett, F. R. *J. Electrochem. Soc.* **2016**, *163*, A5253−A5262.
(33) Doris, S. E.; Ward, A. L.; Baskin, A.; Frischmann, P. D.; Gavvalapalli, N.; Chénard, E.; Sevov, C. S.; Prendergast, D.; Moore, J. S.; Helms, B. A. *Angew. Chem., Int. Ed.* **2017**, *56*, 1595−1599.
(34) Shirman, E.; Ustinov, A.; Ben-Shitrit, N.; Weissman, H.; Iron, M. A.; Cohen, R.; Rybtchinski, B. *J. Phys. Chem. B* **2008**, *112*, 8855−8858.
(35) Huang, C.; Barlow, S.; Marder, S. R. *J. Org. Chem.* **2011**, *76*, 2386−2407.
(36) van Staveren, D. R.; Metzler-Nolte, N. *Chem. Rev.* **2004**, *104*, 5931−5985.
(37) Due to the small separation of the events, the individual $E_{1/2}$ of the first and second events could not be determined.
(38) Lee, S. K.; Zu, Y. B.; Herrmann, A.; Geerts, Y.; Mullen, K.; Bard, A. J. *J. Am. Chem. Soc.* **1999**, *121*, 3513−3520.
(39) In addition, we observed that $LiBF_4$ and $[Et_4N][BF_4]$ dissolved in acetonitrile were able to pass through the membrane.
(40) Wei, X. L.; Xu, W.; Huang, J. H.; Zhang, L.; Walter, E.; Lawrence, C.; Vijayakumar, M.; Henderson, W. A.; Liu, T. B.; Cosimbescu, L.; Li, B.; Sprenkle, V.; Wang, W. *Angew. Chem., Int. Ed.* **2015**, *54*, 8684−8687.
(41) Li, L.; Kim, S.; Wang, W.; Vijayakumar, M.; Nie, Z.; Chen, B.; Zhang, J.; Xia, G.; Hu, J.; Graff, G.; Liu, J.; Yang, Z. *Adv. Energy Mater.* **2011**, *1*, 394−400.
(42) CE = (discharge capacity/charge capacity) × 100%.
(43) Huskinson, B.; Marshak, M. P.; Gerhardt, M. R.; Aziz, M. J. *ECS Trans.* **2014**, *61*, 27−30.
(44) Liu, T.; Wei, X.; Nie, Z.; Sprenkle, V.; Wang, W. *Adv. Energy Mater.* **2016**, *6*, 1501449.
(45) Lin, K.; Gómez-Bombarelli, R.; Beh, E. S.; Tong, L.; Chen, Q.; Valle, A.; Aspuru-Guzik, A.; Aziz, M. J.; Gordon, R. G. *Nat. Energy* **2016**, *1*, 16102.
(46) Wei, X.; Duan, W.; Huang, J.; Zhang, L.; Li, B.; Reed, D.; Xu, W.; Sprenkle, V.; Wang, W. *ACS Energy Lett.* **2016**, *1*, 705−711.
(47) Duan, W.; Huang, J.; Kowalski, J. A.; Shkrob, I. A.; Vijayakumar, M.; Walter, E.; Pan, B.; Yang, Z.; Milshtein, J. D.; Li, B.; Liao, C.; Zhang, Z.; Wang, W.; Liu, J.; Moore, J. S.; Brushett, F. R.; Zhang, L.; Wei, X. *ACS Energy Lett.* **2017**, *2*, 1156−1161.
(48) Connelly, N. G.; Geiger, W. E. *Chem. Rev.* **1996**, *96*, 877−910.
(49) $[PDI][TFSI]_2$ was used for crossover experiments due to its smaller size and strong absorption.

DOI: 10.1021/acs.nanolett.7b04131
Nano Lett. 2017, 17, 7859−7863